A Control Framework to Enable a Commercial Building HVAC System for Energy and Regulation Market Signal Tracking

Wenyi Wang, Guanyu Tian, *Graduate Student Member, IEEE*, Qun Zhou Sun, *Member, IEEE*, and Hongrui Liu

***Abstract*—Commercial buildings are great demand response resources in the energy and regulation markets. Many commercial building heating, ventilation and air conditioning (HVAC) systems are composed of a chiller producing chilled water, and multiple Air-Handling Units (AHUs) distributing cooled air to thermal zones. Demand response of such systems has the potential to closely track energy and regulation market signals. However, existing control methods are mostly focused on fan control, neglecting the impact of the air loop fan control on the power consumption of water loop pumps and chillers. This paper presents a complete modeling of a commercial building HVAC system consisting of chiller, water pump and multiple AHUs, and develops a two-level control to follow five-minute energy market signals and four-second frequency regulation signals. The first-level coarse control provides commands for both water and air loop variables, the second-level fine control adjusts the fan commands while maintaining the water loop inputs within the five-minute control period. As a result, the water-loop power serves as a basis to track energy market signals and the air-loop fan control can be adjusted flexibly for frequency regulation. A high-fidelity model in Dymola is built to validate the model and control. The validation is conducted through co-simulation between Matlab and Dymola model via the Building Controls Virtual Test Bed (BCVTB). The simulation results show significant tracking improvement with the proposed two-level control framework.**

***Index Terms*—Commercial building HVAC system, two-level control, energy and regulation market signal tracking, control-oriented model, Dymola high fidelity model.**

NOMENCLATURE

Variables

P_{total}	Total power consumption of HVAC
$P_{chiller}$	Chiller power consumption
P_{pump}	Pump power consumption
P_{fan}	Fan power consumption
$\dot{m}_{as}$	Supply air mass flow rate
$\dot{m}_{chw}$	Chilled water mass flow rate
P_{ref}	Nominal power consumption of chiller
T_{chws}	Chilled water supply temperature
T_{cws}	Condense water supply temperature
$Q_{chiller}$	Cooling capacity of chiller
Q_{ref}	Nominal cooling capacity of chiller
Q_{coil}	Cooling capacity of cooling coil
T_{chwr}	Chilled water return temperature
c_{water}	Specific heat capacity of water
C_r	Overall thermal capacitance of the room
C_w	Overall thermal capacitance of the wall
T_o	Outdoor ambient temperature
T_w	Wall temperature
T_r	Room/Zone temperature
R_{wo}	Exterior resistances of wall
R_{wi}	Interior resistances of wall
R_{con}	Convective resistance (inner wall/room air)
R_{win}	Resistance of window
R_{conwin}	Convective resistance (inner window/room air)
T_{as}	Supply air temperature
Q_{ig}	Internal heat gain
Q_{rad}	Solar radiation heat gain
C_{water}	Heat capacity of the water
C_{air}	Heat capacity of the air
C_{tube}	Heat capacity of the metal tube
T_{amix}	Mixed temperature of return and outside air
β	Outside air damper opening
x	State vector
u	Input vector
d	Environmental disturbance vector
P^E	Energy market signal
P^{AC}	The actual power consumption of HVAC
ΔP^{FR}	Frequency regulation signal

Subscripts and Superscripts

i	Index of AHU
t	Time index

Manuscript received 28 June 2021; revised 24 November 2021 and 22 January 2022; accepted 26 February 2022. Date of publication 7 March 2022; date of current version 22 December 2022. This work was supported by the U.S. Department of Energy's Office of Energy Efficiency and Renewable Energy (EERE) under the Building Technology Office, BENEFIT 2019 under Award DE-EE0009152. Paper no. TPWRS-01025-2021. *(Corresponding author: Qun Zhou Sun.)*

Wenyi Wang, Guanyu Tian, and Qun Zhou Sun are with the Department of Electrical and Computer Engineering, University of Central Florida, Orlando, FL 32816 USA (e-mail: we857643@ucf.edu; tiang@knights.ucf.edu; qz.sun@ucf.edu).

Hongrui Liu is with the Department of Industrial and Systems Engineering, San Jose State University, San Jose, CA 95192 USA (e-mail: hongrui.liu@sjsu.edu).

Color versions of one or more figures in this article are available at https://doi.org/10.1109/TPWRS.2022.3156867.

Digital Object Identifier 10.1109/TPWRS.2022.3156867

I. Introduction

BUILDINGS and the power grid become increasingly interdependent in recent years. This is partly due to the drastic increase of intermittent renewable energy resources, which requires the grid to be much more flexible to accommodate the uncertainty and variability. As a less expensive alternative to battery systems, smart buildings possess a significant potential for the grid flexibility and thus are great resources to balance electrical supply and demand in real time.

Market rules for Demand Response Resources (DRRs) have been developed in the U.S. wholesale power markets, following FERC order 745 [1]. For example, a new Price-Responsive Demand (PRD) structure went into effect in ISO-NE in 2018 [2]. The new structure allows DRRs to participate in energy and reserve markets with a minimum size of 5MW. The DRRs are expected to follow the grid dispatch signals and get paid at market clearing prices of energy and reserves. In addition, FERC order 755 further specifies the performance-based rules for different resources to provide frequency regulation services. It requires the wholesale power markets to compensate the regulation resources based on their accuracy to follow grid dispatch signals [3].

Commercial buildings are good candidates to participate in energy and regulation markets, because they have fast electrical dynamics to respond to grid signals, while their large thermal inertia results in slow-changing room conditions, which is desired for maintaining occupant comfort. Among all building energy components, the heating, ventilation and air conditioning (HVAC) system in a building dominates the energy consumption [4]. Commercial HVAC systems are commonly composed of a chiller to provide chilled water for heat exchange with the air, and multiple Air-Handling Units (AHUs) to distribute the cooled air to rooms. By adjusting controllable elements such as chilled water setpoint as well as pump and fan speed, the commercial building HVAC system could closely track energy and regulation market signals while satisfying their service functionalities.

Significant research effort has been dedicated to study the interactions between HVAC systems and the power grid. Many works focus on retail distribution systems and utilize the transactive energy concept where HVAC systems minimize energy cost in response to grid pricing signals [5]–[7]. For wholesale power market, several researchers investigated the feasibility of residential and commercial HVAC systems providing grid services including frequency regulation and load balancing. For instance, intra-hour load balancing potential is evaluated in [8]. HVAC providing frequency regulation service have been studied extensively, through HVAC on/off status control [9]–[11] or fan speed control [12]–[16].

The grid applications require detailed HVAC system modeling and control. The modeling of HVAC systems is evolving in the power system research community, from the simplified state-space model with linear temperature equation and linear/binary power model [9], [10], [17], to nonlinear HVAC model involving air-loop heat transfer equations [15], [18]. Depending on the modeling details of the HVAC system, control variables can be HVAC on/off status, room temperature setpoints, and air mass flow rate.

Note that commercial buildings do not only have air-loop heat exchange from thermal zones and fans but also have water-loop heat exchange from chillers and chilled water pumps [19]. In fact, the power consumption of chiller and pumps accounts for 43% of a typical commercial HVAC system, which is greater than the portion from fan energy (34%) [20]. In a realistic HVAC system, fans, pumps, and the chiller are very interdependent through a highly coupled heat exchange process in the air and water loops with commonly-used Proportional-Integral (PI) controls. A change in one control variable could cause changes in other variables. In addition, a chiller with the time-varying Coefficient of Performance (COP) introduces an extra layer of complexity to the system. Nevertheless, a critical research gap exists in the literature where the frequency regulation can be achieved by solely adjusting the fan speed and power in AHUs, without considering the effect of the fan control on the power of the water loop (i.e., chiller and pumps). As a result, the fan-only control may lead to incorrect regulation signal tracking when the entire HVAC system works as a whole participating in the wholesale power market. Neglecting this interdependence would lead to incorrect response to grid signals, leading to potential grid reliability issues should a large number of buildings be deployed.

To tackle these issues, this paper proposes a two-level control framework for a complete HVAC system in commercial building to follow energy and regulation market signals simultaneously. The first-level control is based on a nonlinear Model Predictive Control (MPC) to track energy market signals every 5 minutes. The second-level control further adjusts fan power by changing the air mass flow rate every 4 seconds while keeping water-loop variables constant throughout the entire five-minute period. This two-level control essentially decouples the air loop from the water loop for frequency regulation. Comparing to existing hierarchical control framework in the literature that is mainly focused on adjusting the fan speed to follow ancillary service signals [15], [16], [21], the goal of our two-level control is to simultaneously track the energy market and frequency regulation signals in a look-ahead market environment with the model predictive control at different time intervals. The air loop, water loop, and a more detailed chiller are dynamically coordinated to participate in both energy and frequency markets.

For implementing our proposed control framework, a complete HVAC control-oriented model is developed, which does not only contain air-loop components such as fans and thermal zones, but also models the water-loop components including the chiller, water pumps, and cooling coils. In addition, a Modelica-based high fidelity model is developed in Dymola for the HVAC system. A co-simulation between Dymola and Matlab is implemented to demonstrate the effectiveness of the two-level control towards meeting the energy and regulation market requirement.

This paper addresses a practical and critical issue when commercial building HVAC system provides grid services. The contributions of this paper are as follows:

- A complete commercial building HVAC system control-oriented model is developed, which enables the incorporation of more control variables from both water and air loops.

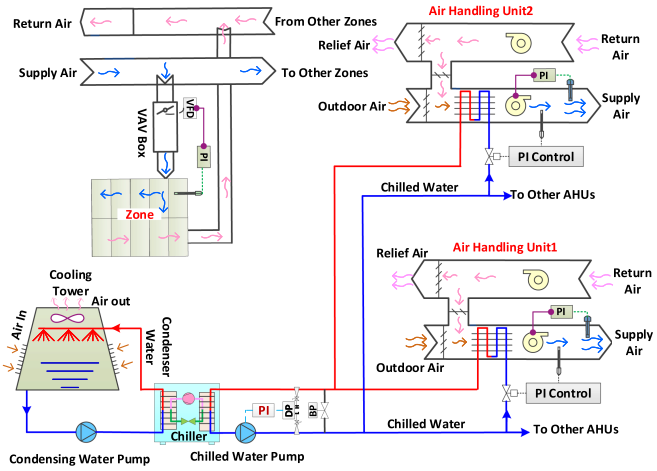

Fig. 1. The schematic diagram of a complete HVAC system in commercial building.

- A two-level control framework is proposed to account for the interdependence of the chiller, pumps, and fans, which successfully decouples water and air loops for closely tracking energy and frequency regulation market signals simultaneously.
- A high-fidelity Dymola model and co-simulation are developed to validate the effectiveness of the two-level control and results show the improvement of tracking performance over a benchmark model and a benchmark control strategy.

The remainder of the paper is organized as follows. Section II presents the problem formulation. The complete control-oriented HVAC model is developed in Section III. Section IV explains controller design and methodology. Section V presents the simulation settings and results. Limitations of the proposed method are discussed in Section VI. Section VII concludes this paper.

II. Problem Formulation

A complete schematic diagram of an HVAC system for commercial buildings is shown in Fig. 1, which consists of a chiller, water pumps, air handling units and a cooling tower system [22]. The cooling load in the buildings is first passed to the chilled water via AHUs. A typical AHU is composed of a cooling coil, a supply and return fan, and dampers. In the AHU, part of the return air is mixed with outside fresh air and passes through the cooling coil where chilled water takes the heat away from the mixed air. The mixed air temperature decreases and is distributed to different zones by the supply fan through ducts and Variable air volume (VAV) boxes. The chilled water temperature increases and returns to the chiller by a chilled water pump. In the chiller, the refrigerant in the evaporator absorbs the cooling load and then transfers it to condenser water by the vapor compression cycle. Finally, the warm condenser water is delivered to the cooling tower, where the cooling load is dumped to the ambient via evaporative cooling.

Such an HVAC system is run via complex control sequences that incorporate PI loops. As shown in the top left corner of Fig. 1, a damper PI controller maintains a room temperature setpoint by adjusting the mass flow rate of inlet cooled air in the VAV box. As different VAV boxes change their damper position to meet the variable local cooling load, the differential pressure across the ducts changes. Based on the pressure setpoint, the supply fan PI controller changes the fan speed via the variable frequency drive (VFD) and thus the total supply air mass flow rate changes. For the chilled water loop, when the supply air mass flow rate changes, each AHU cooling coil PI controller adjusts its valve opening position and changes the inlet chilled water mass flow rate to maintain the supply air temperature setpoint. As different cooling coil valves change, the differential pressure between the supply chilled water pipe and the return water pipe changes. Based on the differential pressure setpoint, then the chilled water pump PI controller changes the pump speed via VFD and hence the water mass flow rate changes. Besides, a bypass valve is installed between the supply water pipe and the return water pump to maintain the minimal water mass flow rate of the evaporator for the chiller's safe operation. For the cooling tower system, the condenser water pump and the cooling tower fan generally operate at a constant speed, which means constant power consumption.

Practically, the operation of the fans, pumps and chiller are highly interdependent. For example, fan power changes would lead to water pump power changes, because different air mass flow rates result in different water mass flow rates. With the changing water mass flow rate, chiller COP is also time-varying. Although frequency regulation can only be conducted by fans, energy market signal tracking should consider the variable total power consumption of fans, pumps, and chillers:

$$P_{total}(t) = P_{fan}(t) + P_{pump}(t) + P_{chiller}(t) \tag{1}$$

Therefore, in this paper, we propose a two-level control strategy to track the power and regulation signal simultaneously. The first level of MPC control can achieve accurate power dispatch signal tracking. Then the MPC result of water-loop variables is fixed throughout the dispatch time window, which successfully decouples the fan power from chiller and pumps power. Now the fan can be used in the second level to track frequency regulation signals.

III. A Complete HVAC System Model With Water and Air Loops

In this section, a complete control-oriented model is developed for a cooling-only HVAC system with chiller, AHUs, and thermal zones in a commercial building. It includes the power model, thermal zone model, cooling coil model, and damper model.

A. Power Model

The power model includes the AHU fan, chilled water pump, and chiller. The fan power consumption P_{fan} is commonly modeled as a third order polynomial of the air mass flow rates $\dot{m}_{as}$ [23]. The chilled water pump power P_{pump} can be modeled similarly as a third order polynomial of the chilled water mass

flow rates $\dot{m}_{chw}$:

$$P_{fan} = \alpha_3 \dot{m}_{as}^3 + \alpha_2 \dot{m}_{as}^2 + \alpha_1 \dot{m}_{as} + \alpha_0 \quad (2)$$

$$P_{pump} = \gamma_3 \dot{m}_{chw}^3 + \gamma_2 \dot{m}_{chw}^2 + \gamma_1 \dot{m}_{chw} + \gamma_0 \quad (3)$$

Where the coefficients α_i, γ_i can be estimated using data collected from building automation systems. Compared to the fan and pump model, the chiller model based on the reversed Carnot cycle and refrigerant properties is too complicated and cannot be suitably incorporated as a control-oriented model. Therefore, to describe chiller characteristics, we adopted the DOE2 electric chiller simulation model, which has been proven with the desired accuracy across a wide range of chiller configurations but with simple structures [24]. In such a DOE2 model, chiller power $P_{chiller}$ is calculated as a function of the nominal power consumption P_{ref} and the current operating conditions represented by three terms.

$$P_{chiller} = CAPFT(T_{chws}, T_{cws}) \times EIRFT(T_{chws}, T_{cws}) \times EIRFPLR(Q_{chiller}, T_{chws}, T_{cws}) \times P_{ref} \quad (4)$$

Note that all terms representing current conditions are functions of chilled water supply temperature T_{chws} and condense water supply temperature T_{cws}. Each term is defined as follows:

1) CAPFT: The available cooling capacity as a function of evaporator and condenser temperatures, empirically expressed by:

$$CAPFT = a_1 + b_1 \times T_{chws} + c_1 \times T_{chws}^2 + d_1 \times T_{cws} + e_1 \times T_{cws}^2 + f_1 \times T_{chws} \times T_{cws} \quad (5)$$

2) EIRFT: The full-load efficiency as a function of evaporator and condenser temperatures by:

$$EIRFT = a_2 + b_2 \times T_{chws} + c_2 \times T_{chws}^2 + d_2 \times T_{cws} + e_2 \times T_{cws}^2 + f_2 \times T_{chws} \times T_{cws} \quad (6)$$

3): EIRFPLR - The efficiency as a function of the percentage unloading by:

$$EIRFPLR = a_3 + b_3 \times PLR + c_3 \times PLR^2 \quad (7)$$

Where $PLR = Q_{chiller}/(Q_{ref} \times CAPFT(T_{chws}, T_{cws}))$. $Q_{chiller}$ and Q_{ref} represent the current and nominal cooling capacity. $Q_{chiller}$ is the summation of the energy consumed by all AHU cooling coils and each cooling coil energy consumption can be formulated by:

$$Q_{coil}^i = \dot{m}_{chw}^i \times c_{water} \times (T_{chwr}^i - T_{chws}) \quad (8)$$

Thus the COP of chiller is the ratio of the chiller cooling capacity $Q_{chiller}$ over the chiller power consumption $P_{chiller}$:

$$COP = \frac{Q_{chiller}}{P_{chiller}} = \frac{\sum Q_{coil}^i}{P_{chiller}} \quad (9)$$

Where $\dot{m}_{chw}^i$ and T_{chwr}^i denote the chilled water mass flow rate and the chilled water return temperature for the water passing through each cooling coil. The chilled water supply temperature T_{chws} is the same for all AHU cooling coils.

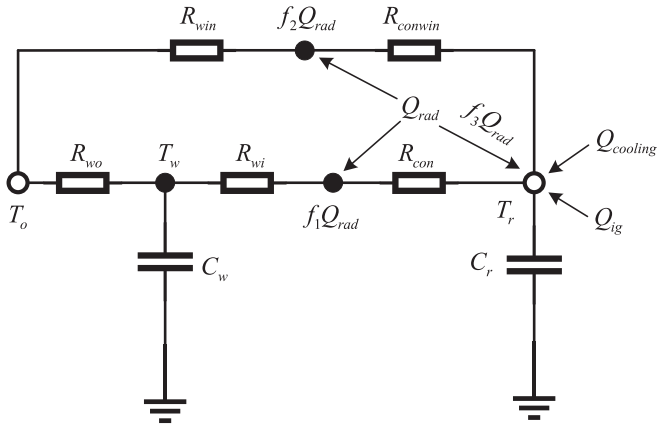

Fig. 2. The schematic diagram of the R-C thermal network.

c_{water} is the specific heat capacity of water. The coefficients (a_i, b_i, c_i, d_i, e_i and f_i) in the three terms can be obtained based on the technique proposed in [24] for well-formed data sets. The total power consumption for the entire HVAC plant is the summation of all fans in AHUs, the chilled water pumps and the chiller.

B. Thermal Zone Model

An R-C thermal network is commonly used to represent the zone dynamics, where two thermal capacitors are used for walls and rooms, and thermal resistances are used for windows and walls [25], [26]. Fig. 2 shows the specific schematic diagram. Solar radiation is distributed to different nodes. It is assumed that the room temperature is uniformly distributed and all walls are aggregated.

In Fig. 2, C_r and C_w are the thermal capacitance of the room and wall. T_o, T_w, T_r is the outdoor ambient temperature, wall temperature, and room temperature. The heat transfer process occurs at the wall and window layers. For the wall layer, R_{wo}, R_{wi} is the exterior and interior resistances, and R_{con} is the convective resistance between the inner wall surface and room air. For the window layer, R_{win} is the window resistance, R_{conwin} is the convective resistance between the inner window and the room air. The inner wall surfaces, inner window surfaces, and room air receive solar radiation, of which the percentages are represented by the coefficients f_1, f_2 and f_3. $Q_{cooling} = \dot{m}_{as} c_{air}(T_{as} - T_r)$ is the cooling capacity provided by the AHU, where $\dot{m}_{as}$ and T_{as} are the supply air mass flow rate and temperature, c_{air} is the specific heat capacity of air. Q_{ig} is the internal heat gain from the human, computer and other plug loads. Based on the energy balance and Kirchhoff's circuit laws, the R-C model can be described as follows:

$$C_r \frac{dT_r}{dt} = \frac{T_o - T_r}{R_{win} + R_{conwin}} + \frac{T_w - T_r}{R_{wi} + R_{con}} + \frac{R_{wi} f_1 Q_{rad}}{R_{wi} + R_{con}} + \frac{R_{win} f_2 Q_{rad}}{R_{win} + R_{conwin}} + f_3 Q_{rad} + Q_{ig} + \dot{m}_{as} c_{air}(T_{as} - T_r) \quad (10)$$

$$C_w \frac{dT_w}{dt} = \frac{T_o - T_w}{R_{wo}} + \frac{T_r - T_w}{R_{wi} + R_{con}} + \frac{R_{con} f_1 Q_{rad}}{R_{wi} + R_{con}} \quad (11)$$

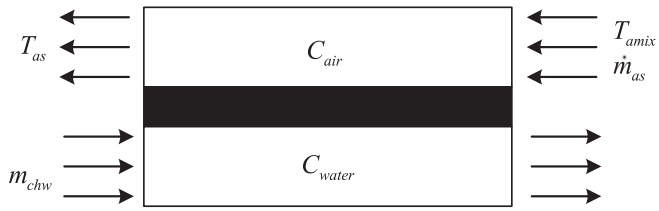

Fig. 3. Heat transfer mechanism in the coil.

Utilizing the explicit Euler method to discretize (10) and (11) yields a set of discrete-time difference equations for the room and wall temperature, which will be integrated into the overall HVAC model in Section III-D.

C. Cooling Coil and Damper Model

An actual cooling coil is designed as a cross counterflow to exchange heat between the chilled water and mixed air. Water passes through the sinuous tube, and air crossly passes through the fins winding around the exterior surfaces of tubes. For the purpose of modeling, it is valid to consider several bent tubes together and as a pure counterflow [27]. However, even with such simplification, the mathematical description of water and air temperature are still partial differential equations of the time and direction, which is difficult to use in the controller. Hence, we assume the following: 1) the water and air flow along the tube in one dimension and can be discretized into multiple segments; 2) the temperature of the flow is the function of time in each segment; 3) the heat capacity of the tube is negligible compared to that of water and air; 4) condensation is not accounted for. Fig. 3 depicts the heat transfer mechanism of the cooling coil. The energy balance equations on one segment can be expressed by:

$$C_{water}\frac{dT_{chwr}}{dt} = h_w(T_{tube}-T_{chwr}) + \dot{m}_{chw}c_{water}(T_{chws}-T_{chwr}) \quad (12)$$

$$C_{air}\frac{dT_{as}}{dt} = h_a(T_{tube}-T_{as}) + \dot{m}_{as}c_{air}(T_{amix}-T_{as}) \quad (13)$$

$$C_{tube}\frac{dT_{tube}}{dt} = h_w(T_{chwr}-T_{tube}) + h_a(T_{as}-T_{tube}) = 0 \quad (14)$$

Where C_{water} and C_{air} is the heat capacity of the water and air in the specific segment, C_{tube} is the heat capacity of the metal tube and equals to zero based on the assumption. h_w is the convective heat transfer coefficient between tube and water, h_a is the convective heat transfer coefficient between tube and air. T_{amix} is the mixed temperature of recirculation and outside air.

For the damper modeling, the damper opening level β is proportional to the ratio of outside air mass flow rate over the mixed supply air mass flow rate $\dot{m}_{as}$. While assuming the mixing process of the recirculation air and outside air is instantaneous, the steady-state equation for the mixed air temperature T_{amix} is written as follows:

$$\dot{m}_{as}\beta c_{air}T_o + \dot{m}_{as}(1-\beta)c_{air}T_r - \dot{m}_{as}c_{air}T_{amix} = 0 \quad (15)$$

D. Overall HVAC Model

(2)–(15) depict the heat dynamics and the power consumption of a commercial building HVAC system. Among these, (14) and (15) are steady equations, so T_{tube} and T_{amix} can be solved and then substituted into (12) and (13). Then discretize (10)–(13) with the Euler method and substitute the constant coefficients in the discretized equations with a_{ij}, b_{ij}, c_{ij}, d_{ij}. Finally, a complete HVAC control-oriented model with water and air loop interdependence can be formulated as a standard matrix format as shown in (16).

$$x_{k+1} = Ax_k + B\hat{u}_k + Cx_k u_{3,k} + Dd_k \quad (16)$$

It is worth noting that the (16) is for one AHU with its thermal zone, in which the states, inputs and disturbances vector are defined as $x = [T_r\ T_w\ T_{chwr}\ T_{as}]^T$, $u = [\dot{m}_{chw}\ T_{chws}\ \dot{m}_{as}\ \beta]^T$ and $d = [T_o\ Q_{rad}\ Q_{ig}]^T$. The $\hat{u} = [\dot{m}_{chw}(T_{chws}-T_{chwr})\ \dot{m}_{as}\beta T_o\ \dot{m}_{as}(1-\beta)T_r\ 0]^T$. The matrices $A\ B\ C\ D$ can be obtained by discretizing the differential equations. For a chiller with multiple AHUs, (16) can easily duplicate for other AHUs, among which the T_{chws} and T_o are the same for all AHUs. Generally, For an HVAC plant, there is usually more than one AHU installed at different sites or on different floors for one building.

IV. A Two-Level Control to Track the Energy and Regulation Market Signals

In real-time economic dispatch, energy and reserves are co-optimized. Look-ahead economic dispatch with multiple time intervals is available in wholesale power markets such as PJM and ISO-NE. Frequency regulation deployment signals are sent every 4 seconds through Automatic Generator Control (AGC). To track energy and regulation market signals simultaneously, the two-level control provides a coarse 5-minute MPC control to follow energy market signals, and a fine 4-second control to adjust fan output for frequency regulation while maintaining the water-loop power consumption within the five-minute time window. This control framework can successfully decouple the power consumption from air loop and water loop, then the control on fans for frequency regulations no longer cause a side-effect on the power consumption of pump and chiller.

A. First-Level Coarse Control: Five-Minute MPC to Track Energy Market Signals

The energy market signal is given every five minutes. To comply with the power dispatch result, the MPC is designed to minimize the deviation between the actual power consumption and the power dispatch signal via the control vector $u = [\dot{m}_{chw}\ T_{chws}\ \dot{m}_{as}\ \beta]^T$. Let P_k^E denote the energy market signal or power dispatch signal at time step k. For simplicity, the power dispatch signals P_k^E used in the paper are direct consumption

signals that can be either decreased or increased from the baseline. Note that the baseline method is a common practice for DRRs to provide demand response in a wholesale power market, and several methods exist to compute the baseline [28]. Once the baseline is established and real-time demand modification (reduction or increase) signals are published in the market, the direct power signals P_k^E can be calculated by subtracting from or adding to the baseline and input into the first-level control framework.

Let P_k^{AC} denote the actual power consumption that comes from the fans, pumps and chiller. According to a previous study [29], chiller ramp rate is constrained by internal PI parameters and mechanical inertia, which is around 3%-5% per minute of the nominal power. This ramp rate is sufficient for tracking 5-minute energy market signals. By adjusting both water-loop and air-loop variables, the commercial HVAC system is designed to track the grid signal closely while maintaining occupant comfort. The five-minute MPC optimization problem can be formulated as follows:

$$\min_{u} \quad \sum_{j=1}^{N} (P_{k+j}^{AC} - P_{k+j}^{E})^2 \tag{17a}$$

s.t. $for \quad j = 1:N,$

$$P_{k+j}^{AC} = P_{fan,k+j} + P_{pump,k+j} + P_{chiller,k+j} \tag{17b}$$

$$x_{k+j} = Ax_{k+j-1} + B\hat{u}_{k+j-1} + Cx_{k+j-1}u_{3,k+j-1} + Dd_{k+j-1} \tag{17c}$$

$$T_{r,min} \le T_{r,k+j} \le T_{r,max} \tag{17d}$$

$$x_{min} \le x_{k+j} \le x_{max} \tag{17e}$$

$$u_{min} \le u_{k+j} \le u_{max} \tag{17f}$$

$$\Delta u_{min} \le \Delta u_{k+j} \le \Delta u_{max} \tag{17g}$$

Where N is the prediction horizon. $T_{r,min}$ and $T_{r,max}$ are lower and upper bounds of room temperature. The states x_{k+j} and inputs u_{k+j} are all limited by the preset upper and lower bounds. T_{chws}, T_{chwr} and T_{as} are limited by the chiller and cooling coil size, which should not exceed the maximum chiller capacity. To ensure sufficient ventilation, a mimum damper opening β_{min} should be set. The changes in control actions Δu_{k+j} should be bounded to prevent dramatic changes in operations of HVAC components in two consecutive steps. Note that all the preset upper and lower limits can be changed based on the cooling load conditions. This nonlinear optimization problem can be solved by the 'IPOPT' solver using interior point method [30].

B. Second Level Fine Control: 4-Second Mass Flow Rate Control to Track Frequency Regulation Signals

While keeping the chiller and water pump power constant in the first level of control, the second level of control utilizes the fan to track frequency regulation signals, which requires a fast ramping rate. According to a previous study [31], the fan ramp rate, constrained by fan size and mechanical inertia, is around 18% of nominal power per second. This ramp rate is sufficient for tracking 4-second frequency regulation signals. Maintaining the first-level water-loop variables is essential to ensure that only the fan power changes contribute to the entire HVAC system power change. As a result, the power consumption of fans is successfully decoupled from that of the pumps and chiller, leading to an accurate energy and regulation market signal tracking simultaneously. Note that ramp rates for both the chiller and fan are all case dependent and possibly time-varying.

Algorithm 1: Frequency Regulation Fan Control.

Input: $\dot{m}_{as,i}$, ΔP^{FR}
Output: $\dot{m}_{as,i}^{FR}$
for *t = 1 to 75* **do**
  Evaluate reference fan powers $P_{fan,i}^{ref}, \forall i$ by (2);
  Dispatch FR signal $\Delta P_i^{FR} = \Delta P^{FR} \frac{P_{fan,i}^{ref}}{\sum_{i=1}^{N} P_{fan,i}^{ref}}$;
  Solve $\dot{m}_{as,i}^{FR}$ from (2) = $P_{fan,i}^{ref} + \Delta P_i^{FR}$;
  Return $\dot{m}_{as,i}^{FR}$;

The response strategy of frequency regulation in the second level is formulated in Algorithm 1, where $\dot{m}_{as,i}$ is the supply air mass flow rate command from the first level of 5-minute control, used as a reference point to determine the allocation of adjusted regulation power to each AHU. The mass flow rate of fan is adjusted every 4 seconds based on the current AGC signal until the arrival of the next signal. The number of 4-second intervals in a 5-minute window is 75. The frequency regulation signal ΔP^{FR} is proportionally distributed among all fans. The individual fan power adjustment is denoted by ΔP_i^{FR}. The response air mass flow rates $\dot{m}_{as,i}^{FR}$ can be transferred to the fan speed and sent to the fan VFD.

V. Numerical Results

When the proposed control strategy is applied in a realistic building, the system outputs are measured by building sensors and then fed back to the controller. To mimic the real-time situation, we build a high-fidelity physical model approximating the real HVAC system, and the two-level control strategy is applied in the physical model by co-simulation. The two-level control framework with the proposed HVAC model is compared with a benchmark model and control strategy.

A. High-Fidelity Physical Model and Simulation Settings

The high-fidelity physical model is built in the Dymola [32] platform using the Building library [33] as shown in Fig. 4. The HVAC system is designed with one chiller, one water pump and two AHUs, the cooling tower system is replaced by the constant boundary conditions. Each AHU includes a cooling coil, one supply and return fan, and a mixing box. Each AHU serves an independent thermal zone. The two independent thermal zones have the same construction but different solar radiation and internal gains. A realistic ambient temperature can be obtained from the TYM3 weather data source [34]. A self-built solar

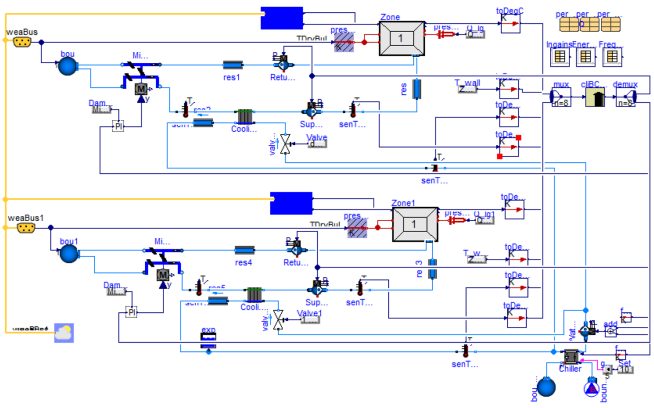

Fig. 4. The layout of the HVAC system in Dymola.

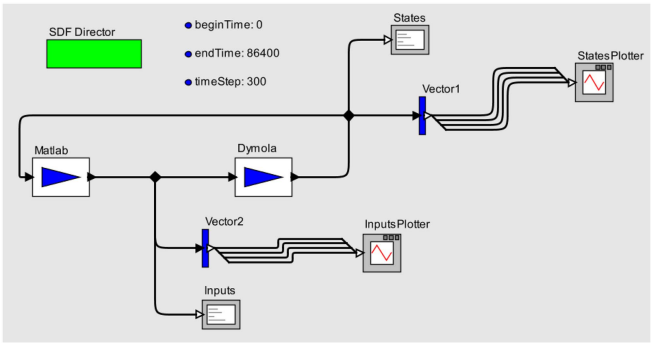

Fig. 5. The layout of co-simulation between Matlab and Dymola.

radiation module based on the other library components can produce practical solar radiation. According to the research in [35], the internal gain in commercial buildings can be considered as piecewise constant, so a piecewise constant internal heat gain based on the ASHRAE Table 8.19 [36] is adopted for each zone.

The two-level control algorithm is applied online in this Dymola model via co-simulation between the controller in Matlab and Dymola using the Building Controls Virtual Test Bed (BCVTB) [37]. The specific layout of the flow chart is shown in Fig. 5. It should be mentioned that the model built in Dymola is composed of different modules developed by the Modelica Buildings Library, which has higher fidelity than the control-oriented model developed in Section III. This Dymola plant is used in the co-simulation to validate the proposed control-oriented HVAC model and the proposed two-level control strategy. The operating states $x = [T_r\ T_w\ T_{chwr}\ T_{as}]^T$ are measured from the Dymola model and sent to the controller in Matlab, and then the decision variables $u = [\dot{m}_{chw}\ T_{chws}\ \dot{m}_{as}\ \beta]^T$ are computed and sent back to the physical model.

The total states and inputs are eight in this simulation due to two AHUs involved in the simulation. For the air loop, the controller provides the respective air mass flow rate of the fan and damper opening for each AHU. For the water loop, the controller provides the respective chilled water mass flow rate for each AHU cooling coil, and a linear valve is used to assign the calculated value in Dymola. The water mass flow rate that passes through the water pump is the summation of the two. The chilled water supply temperature is the same for both two AHUs. In this co-simulation, the sampling rate is every 5 minutes and the prediction horizon is 20 minutes, i.e., 4 timesteps. The bounds of physical constraints for two AHU are same, they are: $T_r \in [19\ 26]$, $T_{as} \in [10\ 20]$, $\dot{m}_{chw} \in [2\ 20]$, $T_{chws} \in [4\ 9]$, $\dot{m}_{as} \in [5\ 30]$, and $\beta \in [0.3\ 1]$.

B. Benchmark HVAC Model

A simple HVAC model is developed to compare with the control-oriented model. In the benchmark model, the chilled water mass flow rate is constant, which means a constant chilled water pump consumption. The chilled water supply temperature and the outside air ratio are also constant. The chiller power consumption is calculated below:

$$P_{chiller} = \frac{Q_{chiller}}{COP_{nom}} = \frac{\dot{m}_{as} c_{air} (T_{amix} - T_{as})}{COP_{nom}} \tag{18}$$

Where the chiller COP under nominal condition COP_{nom} is adopted. The cooling capacity is directly calculated from the air loop, so the cooling coil model is not needed. The thermal zone model is the same as that in the proposed model. Both models are compared through co-simulation between Matlab and BCVTB with the same first-level MPC control, and the same disturbances are adopted. Consequently, in the benchmark model, the air mass flow rate of the fan in AHUs is the only variable to be adjusted.

C. Benchmark Control Strategy

The proposed control framework is compared with a benchmark control strategy, to validate the effectiveness of the two-level control. In the benchmark control strategy, the air mass flow rate $\dot{m}_{as}$ that passes through the fan in each AHU is the same as that in the proposed two-level control to track the 4-second frequency regulation signal, while the water mass flow rate $\dot{m}_{chw}$ is adjusted by the conventional PI control as introduced in Section II. The PI reference setpoint of supply air temperature T_{as} is set to a constant 16 °C for both AHUs, the chilled water supply temperature T_{chws} is set to a constant 7 °C. The ratio of outside air mass flow rate over the mixed air mass flow rate β is set to a constant 0.3. The benchmark control strategy and proposed two-level control are applied in the Dymola model with the same disturbances.

D. Energy Market Signal Tracking With the Proposed and Benchmark Models

In the following two sections, we describe the simulation results of tracking a 5-minute energy market signal with the proposed and benchmark models, and a 4-second frequency regulation signal with the two-level and benchmark control strategy. All simulations are conducted under the same disturbances as shown in Fig. 6, which includes a real-time 24-hour ambient temperature, solar radiation, and internal gain. The power dispatch signal and frequency regulation signal are both taken from the ISO New England website [38]. They are then scaled down so that their magnitude is close to the total power consumption and fan power consumption respectively.

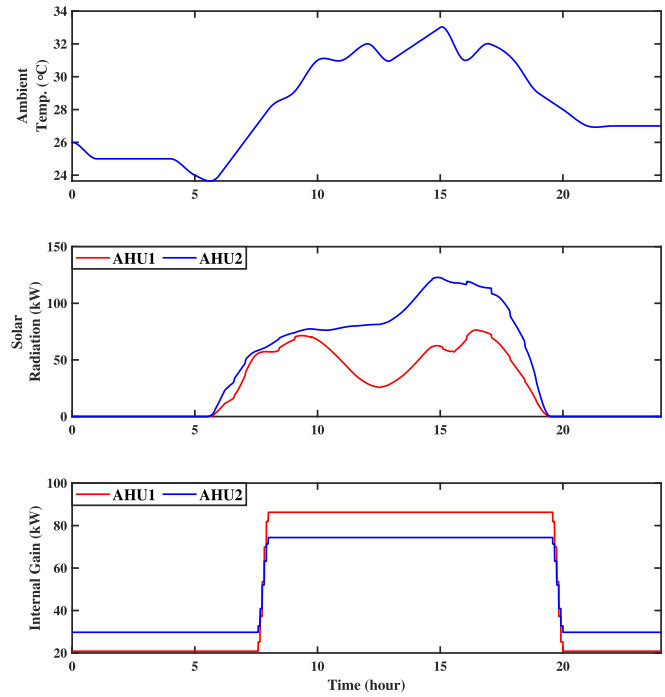

Fig. 6. Ambient temperature, solar radiation and internal gain profiles.

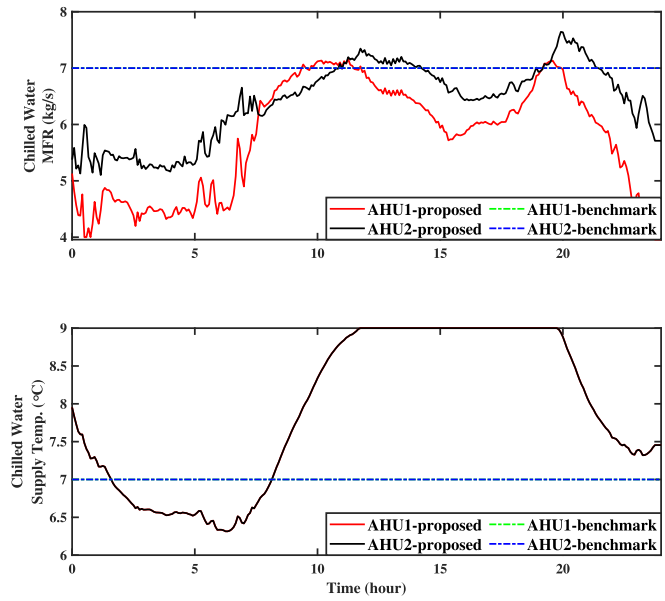

Fig. 7. The profiles of chilled water mass flow rate (MFR) and chilled water supply temperature in the proposed and benchmark model.

The proposed complete HVAC model is first compared with the benchmark model under the first-level MPC control through co-simulation. Fig. 7 shows the profile of the chilled water mass flow rate and chilled water supply temperature. It is seen that in the benchmark model, the two variables are set to constants, leading to a reduced number of control variables. In the proposed HVAC model, the controller provides optimal chilled water mass flow rate and temperature.

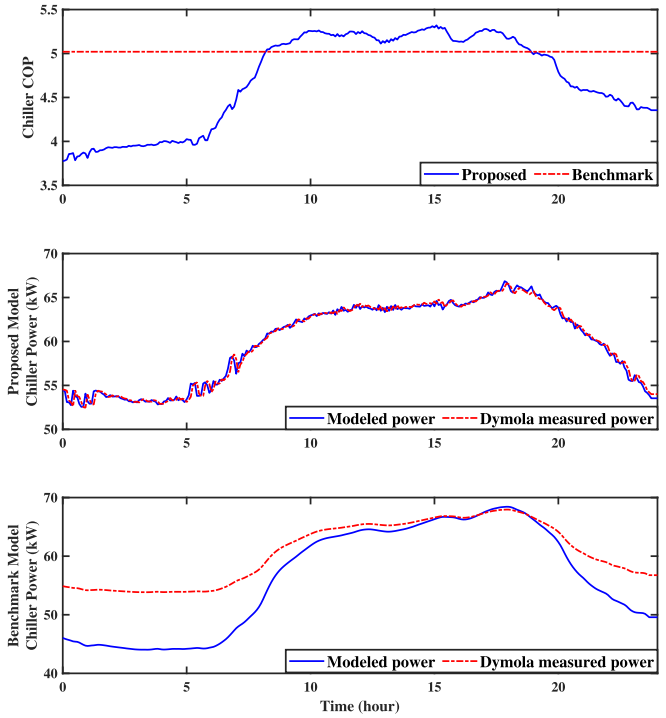

Fig. 8. The profiles of chiller COP and power consumption in the proposed and benchmark model.

TABLE I
THE RMSE COMPARISON BETWEEN DIFFERENT MODELS

Model	Proposed	Benchmark
RMSE	0.49	5.94

Fig. 8 compares the COP for two models: a constant nominal COP is used in (18) to calculate the chiller power in the benchmark model and the time-varying COP is the operating result in the proposed model. The observation of time-varying COP indicates that using a nominal COP may not be sufficiently accurate for approximating chiller power. This can be seen from the modeled and measured chiller power consumption in the two bottom subfigures. Applying the MPC on both the proposed and the benchmark models, two sets of control variables are sent to the same Dymola building model to obtain realistic power measurement. It can be clearly seen that for the proposed HVAC model, the modeled chiller power is very close to the realistic operating result in Dymola, but the power consumption of the benchmark model deviates considerably from Dymola power measurement. The Root Mean Squared Error (RMSE) for the proposed and benchmark model is 0.31 and 5.92 respectively.

Fig. 9 compares the simulation results of the fan air mass flow rate and the 5-minute energy market signal tracking between the proposed model and the benchmark model. For illustration purposes, only the fan in AHU1 is shown and AHU2 has a similar pattern. It can be clearly seen that the proposed HVAC model can closely track the energy market signal, but the benchmark model fails to do so. The RMSE of the tracking accuracy for the proposed and benchmark model is 0.49 and 5.94 respectively as shown in Table I. In addition, it is observed that the fan

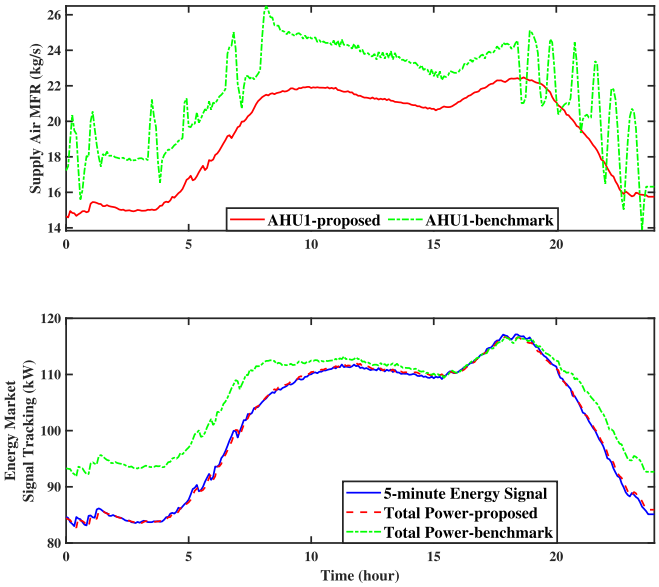

Fig. 9. The profiles of supply air mass flow rate (MFR) and 5-minute energy market signal tracking in the proposed and benchmark model.

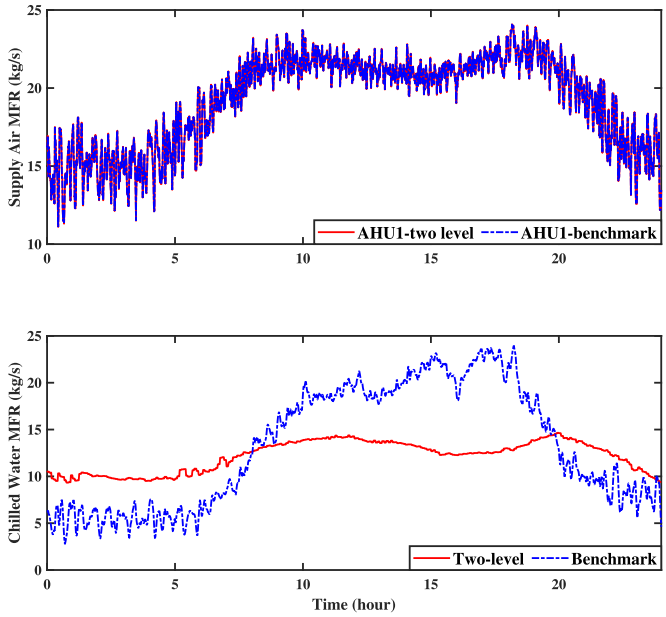

Fig. 10. The profiles of the supply air mass flow rate (MFR) and chilled water mass flow rate with the two-level and benchmark control strategy.

operates smoothly under the proposed model, but is cycling significantly using the benchmark model. The fluctuation magnitude of fans is correlated with the tracking errors. For example, in the benchmark model, when the actual power consumption deviates significantly from the grid signal at around $t \in [0\ 10]$ and $t \in [18\ 24]$, the fan frequently cycles trying to close the gap between the two under the MPC control. This cycling phenomenon is less severe when $t \in [10\ 18]$, due to the reduced tracking errors. In contrast, the fan operates smoothly under the proposed model thanks to small tracking errors. Note that in both cases, the fan control command Δu between two consecutive steps are the same for both models to prevent the abrupt changes of fans. The significantly better tracking performance using the complete HVAC model indicate that using the fan alone is not suitable to track energy market signals, when chiller and pumps provide a large portion of 5-minute power tracking.

It is also worth mentioning that in the benchmark model, the constant setpoints in the water loop are set conservatively to ensure occupant comfort under various operating conditions, e.g., when ambient temperature or solar radiation is high. The conservative settings lead to reduced energy efficiency and higher energy consumption compared to the complete control of both the water and air loops. As shown in Fig. 9, the power consumption in the benchmark model during light cooling period (i.e., morning and night time) is higher than controlling both the water and air loops using the proposed complete HVAC model.

E. Frequency Regulation Signal Tracking With the Two-Level and Benchmark Control Strategies

The proposed two-level control strategy is now compared with the benchmark control strategy using the same Dymola model to track a 4-second frequency regulation signal along with 5-minute power signal. Fig. 10 shows the profile of AHU fan air mass flow rate and the chilled water mass flow rate. Note that the air mass flow rates are the same for both control methods using Algorithm 1 given the same frequency regulation signal. It can be clearly seen that, with the benchmark control, the chilled water mass flow rate is significantly impacted by the fan control of the air loop. To maintain the predetermined constant supply air temperature under the changing air mass flow rate, the internal PI controller adjusts the chilled water mass flow rate frequently. However, the proposed two-level control operates the chilled water mass flow rate smoothly because the first-level MPC control fixes the water-loop variables in the 5-minute time window. In addition, it is observed that the water mass flow rate operate in a much larger range for the benchmark control compared to the two-level control, because the water mass flow rate is the only variable to be adjusted in the benchmark control to meet the supply air temperature setpoint, while the two-level control can adjust both the chilled water supply temperature for the chiller and the chilled water mass flow rate via water pump speed.

The effect of fan control on the power of the water pump and chiller is more clearly seen in Fig. 11, which zooms in a 30-minute time window to show the power consumption from the AHU fans, water pump, and chiller. The fan power is the same for both control strategies due to the same air mass flow rate adopted. However, the water pump and chiller operate differently. The water pump power and chiller power under benchmark control show continuous changes and large variations when the fan power adapts to track the regulation signal. However, in the two-level control framework, the first-level MPC well maintains the water-loop power consumption within the 5-minute time window. Hence, the air mass flow rate changes caused by the AHU fan control do not affect the water loop, ensuring accurate power dispatch signal tracking while providing the frequency regulation. Note that that chiller power is not as strictly maintained as is for the water pump power. This is because the chiller

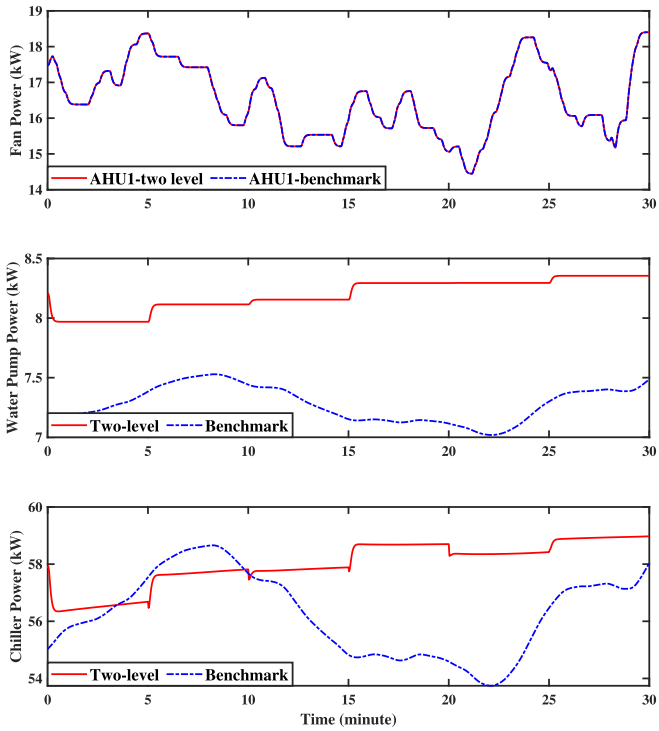

Fig. 11. The profiles of the fan, pump and chiller power consumption with the two-level and benchmark control strategy.

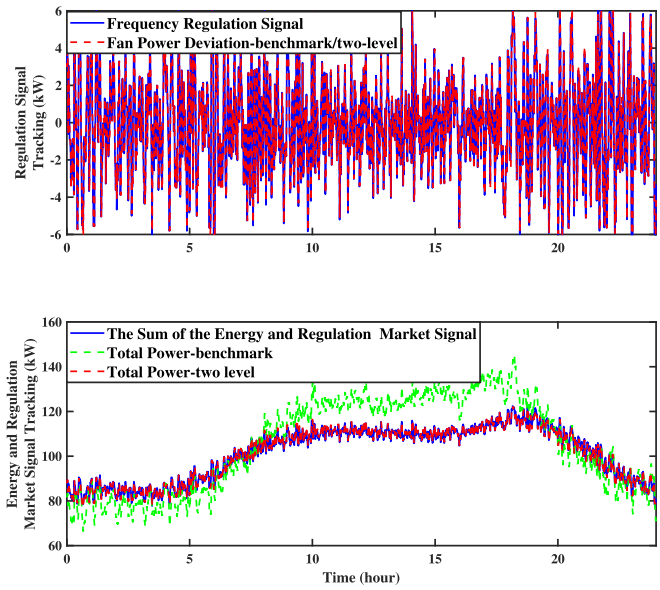

Fig. 12. The profiles of energy and frequency regulation market signal tracking with the two-level and benchmark control strategy.

power consumption is affected by both the water mass flow rate and water temperature which has large inertia. The model mismatch between the proposed control-oriented model and the Dymola model may also contribute to the difference.

Fig. 12 compares the performance of the energy and frequency regulation market signal tracking between the two control strategies. It is observed that, while the fan control can well track the frequency signal, the whole power and regulation signal tracking need to be achieved by coordinating the entire HVAC system including fans, pump and chiller. The proposed two-level control successfully outperforms the benchmark control to track both power and frequency signals simultaneously. The RMSE for the two-level and benchmark control is 0.58 and 10.8 respectively as shown in Table II. The room temperature deviation is within the 0.05 °C for both control strategies. Fig. 12 further indicates that the HVAC power is much more volatile with the internal PI control than the two-level control, due to continuously changing water-loop variables. In addition, the two-level control imposes strict bounds on constraints, which also contributes to the smoothness of the power curve.

TABLE II
THE RMSE COMPARISON BETWEEN DIFFERENT CONTROLS

Control	Two-level	Benchmark
RMSE	0.58	10.8

VI. DISCUSSIONS

In this paper, a two-level control framework is proposed for a complete HVAC system in a commercial building to track the grid energy and regulation market signals, and the simulation results demonstrate the effectiveness of the proposed control framework. Nevertheless, limitations exist and improvements can be made in future research.

First, the HVAC system in real buildings is operated via complex control sequences, including procedures such as the startup, flush, and different modes of operations, with the PI control being part of the control sequence. The proposed control strategy only considers providing an alternative for the PI control to better track the energy and regulation market signals.

Second, although a complete HVAC model in commercial buildings is developed, several simplifications are made in the proposed model. For example, infiltration is not considered in the thermal zone model, condensation is not considered in the cooling coil model, and solar radiation and environmental radiation are lumped together. These simplifications help reduce the number of system states, and thus improve the computational efficiency for the two-level control. Nevertheless, incorporating more realistic conditions in future research could further improve the model accuracy.

Finally, in our case study each AHU serves an independent thermal zone, which is also an uncommon scenario. In real buildings, one AHU connects to multiple VAV boxes that serve different thermal zones. In this paper, the two-level control is focused on the interdependence of the water and air loop but VAV boxes are not considered. A more detailed control framework integrating the top layer coarse control and the terminal VAV box control can further enhance the grid signal tracking performance and the feasibility of the application in realistic buildings.

VII. CONCLUSION

In this paper, a two-level control framework is proposed for a commercial building HVAC system to track energy and regulation market signals. The two-level control essentially decouples

the water loop and air loop when following 5-minute power dispatch signals and 4-second frequency regulation signals. The first level implements a five-minute nonlinear MPC by optimizing the chilled water mass flow rate, the chilled water supply temperature, the air mass flow rate, and damper opening. In the second level, a 4-second control only controls the fan while keeping all water-loop variables the same, so the power change would only come from the fans. To implement such a control framework, a complete control-oriented HVAC system model is developed, which integrates air-loop in AHUs, water loop and chiller. The model is expressed as a matrix with four states and four control variables. Finally, a high-fidelity physical model is built in Dymola, and a co-simulation between the controller and Dymola model is conducted to validate the effectiveness of the proposed control framework. The simulation results show that the developed complete HVAC model permits higher dimensions of controls, which more accurately models HVAC responses compared to the benchmark model. The proposed two-level control strategy results in significantly better performance in grid signal tracking compared to the benchmark control strategy. The limitations of the work are also discussed to provide possible future research directions.

ACKNOWLEDGMENT

The views expressed herein do not necessarily represent the views of the U.S. Department of Energy or the United States Government.

REFERENCES

[1] FERC, "FERC 745: Demand response compensation in organized wholesale energy markets," [Online]. Available: https://www.ferc.gov/sites/default/files/2020-06/Order-745.pdf
[2] ISO New England, "Price responsive demand," [Online]. Available: https://www.iso-ne.com/markets-operations/markets/forward-capacity-market/fcm-participation-guide/price-responsive-demand
[3] FERC, "FERC 755: Frequency regulation compensation in the organized wholesale power markets," [Online]. Available: https://www.ferc.gov/sites/default/files/2020-06/OrderNo.755.pdf
[4] E. I. Administration, "Annual energy outlook 2020." [Online]. Available: https://www.eia.gov/outlooks/aeo/
[5] H. Hao, C. D. Corbin, K. Kalsi, and R. G. Pratt, "Transactive control of commercial buildings for demand response," *IEEE Trans. Power Syst.*, vol. 32, no. 1, pp. 774–783, Jan. 2017.
[6] J. H. Yoon, R. Baldick, and A. Novoselac, "Dynamic demand response controller based on real-time retail price for residential buildings," *IEEE Trans. Smart Grid*, vol. 5, no. 1, pp. 121–129, Jan. 2014.
[7] G. Tian, S. Faddel, Q. Zhou, Z. Qu, and A. Parlato, "Optimal coordination of HVAC scheduling for commercial buildings," in *Proc. IEEE Texas Power Energy Conf.*, 2020, pp. 1–5.
[8] N. Lu, "An evaluation of the HVAC load potential for providing load balancing service," *IEEE Trans. Smart Grid*, vol. 3, no. 3, pp. 1263–1270, Sep. 2012.
[9] X. Wu, J. He, Y. Xu, J. Lu, N. Lu, and X. Wang, "Hierarchical control of residential HVAC units for primary frequency regulation," *IEEE Trans. Smart Grid*, vol. 9, no. 4, pp. 3844–3856, Jul. 2018.
[10] Q. Shi, F. Li, G. Liu, D. Shi, Z. Yi, and Z. Wang, "Thermostatic load control for system frequency regulation considering daily demand profile and progressive recovery," *IEEE Trans. Smart Grid*, vol. 10, no. 6, pp. 6259–6270, Nov. 2019.
[11] S. C. Ross, G. Vuylsteke, and J. L. Mathieu, "Effects of load-based frequency regulation on distribution network operation," *IEEE Trans. Power Syst.*, vol. 34, no. 2, pp. 1569–1578, Mar. 2019.
[12] H. Hao, Y. Lin, A. S. Kowli, P. Barooah, and S. Meyn, "Ancillary service to the grid through control of fans in commercial building HVAC systems," *IEEE Trans. Smart Grid*, vol. 5, no. 4, pp. 2066–2074, Jul. 2014.
[13] Y. Lin, P. Barooah, S. Meyn, and T. Middelkoop, "Experimental evaluation of frequency regulation from commercial building HVAC systems," *IEEE Trans. Smart Grid*, vol. 6, no. 2, pp. 776–783, Mar. 2015.
[14] I. Beil, I. Hiskens, and S. Backhaus, "Frequency regulation from commercial building HVAC demand response," in *Proc. IEEE*, vol. 104, no. 4, pp. 745–757, 2016.
[15] E. Vrettos, E. C. Kara, J. MacDonald, G. Andersson, and D. S. Callaway, "Experimental demonstration of frequency regulation by commercial buildings–Part I: Modeling and hierarchical control design," *IEEE Trans. Smart Grid*, vol. 9, no. 4, pp. 3213–3223, Jul. 2018.
[16] E. Vrettos, E. C. Kara, J. MacDonald, G. Andersson, and D. S. Callaway, "Experimental demonstration of frequency regulation by commercial buildings–Part II: Results and performance evaluation," *IEEE Trans. Smart Grid*, vol. 9, no. 4, pp. 3224–3234, Jul. 2018.
[17] L. Fabietti, T. T. Gorecki, F. A. Qureshi, A. Bitlislioğlu, I. Lymperopoulos, and C. N. Jones, "Experimental implementation of frequency regulation services using commercial buildings," *IEEE Trans. Smart Grid*, vol. 9, no. 3, pp. 1657–1666, May 2018.
[18] J. Wang, S. Huang, D. Wu, and N. Lu, "Operating a commercial building HVAC load as a virtual battery through airflow control," *IEEE Trans. Sustain. Energy*, vol. 12, no. 1, pp. 158–168, Jan. 2021.
[19] K. Deng *et al.*, "Model predictive control of central chiller plant with thermal energy storage via dynamic programming and mixed-integer linear programming," *IEEE Trans. Automat. Sci. Eng.*, vol. 12, no. 2, pp. 565–579, Apr. 2015.
[20] Department of Industry, Science, Energy, and Resources, Australian government. HVAC energy breakdown. [Online]. Available: https://www.energy.gov.au/sites/default/files/hvac-factsheet-energy-breakdown.pdf
[21] Y. Lin, P. Barooah, and J. L. Mathieu, "Ancillary services through demand scheduling and control of commercial buildings," *IEEE Trans. Power Syst.*, vol. 32, no. 1, pp. 186–197, Jan. 2017.
[22] B. Mu, Y. Li, J. M. House, and T. I. Salsbury, "Real-time optimization of a chilled water plant with parallel chillers based on extremum seeking control," *Appl. Energy*, vol. 208, pp. 766–781, Dec. 2017.
[23] M. Stewart, *Surface Production Operations: Volume IV: Pumps and Compressors*. Houston, Texas USA: Gulf Professional Publishing, 2018.
[24] M. Hydeman, K. L. Gillespie, and A. Dexter, "Tools and techniques to calibrate electric chiller component models," *ASHRAE Trans.*, vol. 108, no. 1, pp. 733–741, 2002.
[25] J. H. Kämpf and D. Robinson, "A simplified thermal model to support analysis of urban resource flows," *Energy buildings*, vol. 39, no. 4, pp. 445–453, Apr. 2007.
[26] M. Lauster, J. Teichmann, M. Fuchs, R. Streblow, and D. Mueller, "Low order thermal network models for dynamic simulations of buildings on city district scale," *Building Environ.*, vol. 73, pp. 223–231, Mar. 2014.
[27] Y. Yao and S. Liu, "The transfer function model for dynamic response of wet cooling coils," *Energy Convers. Manage.*, vol. 49, no. 12, pp. 3612–3621, Dec. 2008.
[28] ISO-NE, [Online]. Available: https://www.iso-ne.com/static-assets/documents/2017/02/mmvdr_measurement-and-verification-demand-reduction_rev6_20140601.pdf
[29] L. Su and L. K. Norford, "Demonstration of HVAC chiller control for power grid frequency regulation-Part II: Discussion of results and considerations for broader deployment," *Sci. Technol. Built Environ.*, vol. 21, no. 8, pp. 1143–1153, 2015.
[30] "Ipopt documentation." [Online]. Available: https://coin-or.github.io/Ipopt/
[31] M. Maasoumy, J. Ortiz, D. Culler, and A. Sangiovanni-Vincentelli, "Flexibility of commercial building HVAC fan as ancillary service for smart grid," 2013, *arXiv:1311.6094*.
[32] D. Systèmes, "Multi-engineering modeling and simulation based on modelica and fmi," 2020. [Online]. Available: https://www.3ds.com/products-services/catia/products/dymola/
[33] M. buildings library, "Open source library for building and district energy and control systems," 2020. [Online]. Available: https://simulationresearch.lbl.gov/modelica/
[34] S. Wilcox and W. Marion, "Users manual for tmy3 data sets," 2008.
[35] A. R. Coffman and P. Barooah, "Simultaneous identification of dynamic model and occupant-induced disturbance for commercial buildings," *Building Environ.*, vol. 128, pp. 153–160, Jan. 2018.
[36] A. Handbook, *HVAC Syst. Equip.*, vol. 39, ch. 1996.
[37] L. B. N. Laboratory, "Building controls virtual test bed," 2016. [Online]. Available: https://simulationresearch.lbl.gov/bcvtb/FrontPage
[38] I. N. England, "Real-time maps and charts," 2020. [Online]. Available: https://www.iso-ne.com/isoexpress/

Wenyi Wang received the Ph.D. degree in mechanical engineering from the University of Texas at Dallas, Dallas, TX, USA, in 2019. He is currently a Postdoctoral Researcher with the Department of Electrical and Computer Engineering, University of Central Florida, Orlando, FL, USA. His research interests include HVAC system modeling and optimization, demand response in smart buildings, and advanced control strategies development and application in heat pumps.

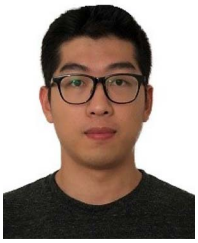

Guanyu Tian (Graduate Student Member, IEEE) received the B.Sc. degree in electrical engineering from Shandong University, Jinan, China, in 2015, and the M.S. degree in electrical engineering from Rensselaer Polytechnic Institute, Troy, NY, USA, in 2016. He is currently working toward the Ph.D. degree with the University of Central Florida, Orlando, FL, USA. His research interests include modeling and optimization of energy systems, demand response, and state estimation.

Qun Zhou Sun (Member, IEEE) received the Ph.D. degree in electrical engineering from Iowa State University, Ames, IA, USA. She is currently an Assistant Professor with the University of Central Florida (UCF), Orlando, FL, USA. She is also the Director of Smart Infrastructure Data Analytics Lab, UCF. Before joining UCF, she was a Power System Engineer with Genscape and GE Grid Solutions. She is dedicated to the research that improves energy sustainability, resiliency, and security. Her research interests include grid-edge resources, including smart buildings, rooftop PVs, and batteries, and their interactions with the grid.

Hongrui Liu received the Ph.D. degree from Industrial and Systems Engineering Department, University of Washington, Seattle, WA, USA, in 2010. She is currently an Assistant Professor with Industrial and Systems Engineering Department, San Jose State University, San Jose, CA, USA. Her primary research interests include optimization modeling, computing algorithms, data analytics, machine learning, and artificial intelligence and their applications in supply chain and energy industry.